Differential Gene Expression Shows Natural Brominated Furanones Interfere With the Autoinducer-2 Bacterial Signaling System of *Escherichia coli*

Dacheng Ren,[1]* Laura A. Bedzyk,[2] Rick W. Ye,[2] Stuart M. Thomas,[2] Thomas K. Wood[1]

[1]Departments of Chemical Engineering and Molecular & Cell Biology, University of Connecticut, 191 Auditorium Road, U-3222, Storrs, Connecticut 06269-3222; telephone: 860-486-2483; fax: 860-486-2959; e-mail: twood@engr.uconn.edu
[2]Experimental Station E328/B33, DuPont Central Research and Development, Wilmington, Delaware

Received 22 April 2004; accepted 8 July 2004

Published online 6 October 2004 in Wiley InterScience (www.interscience.wiley.com). DOI: 10.1002/bit.20259

Abstract: The quorum sensing disrupter (*5Z*)-4-bromo-5-(bromomethylene)-3-butyl-2(*5H*)-furanone (furanone) of the alga *Delisea pulchra* was previously found by us (*Environ Microbiol* 3:731–736, 2001) to inhibit quorum sensing in *Escherichia coli* via autoinducer-2 (AI-2, produced by LuxS). In this study, DNA microarrays were used to study the genetic basis of this natural furanone inhibition of AI-2 signaling (significant values with $p < 0.05$ are reported). Using DNA microarrays, the AI-2 mutant *Escherichia coli* DH5α was compared with the AI-2 wild-type strain, *E. coli* K12, to determine how AI-2 influenced gene expression. *Escherichia coli* K12 was also grown with 0 and 60 μg/mL furanone to study the inhibition of quorum sensing gene expression. It was found that 166 genes were differentially expressed by AI-2 (67 were induced and 99 were repressed) and 90 genes were differentially expressed by furanone (34 were induced and 56 were repressed). Importantly, 79% (44 out of 56) of the genes repressed by furanone were induced by AI-2, which indicated that furanone inhibited AI-2 signaling and influenced the same suite of genes as a *regulon*. Most of these genes have functions of chemotaxis, motility, and flagellar synthesis. Interestingly, the aerotaxis genes *aer* and *tsr* were discovered to be induced by AI-2 and repressed by furanone. Representative microarray results were confirmed by RNA dot blotting. Furthermore, the *E. coli* air–liquid interface biofilm formation was repressed by furanone, supporting the results that taxis and flagellar genes were repressed by furanone. The autoinducer bioassay indicated that 100 μg/mL furanone decreased the extracellular concentration of AI-2 2-fold, yet *luxS* and *pfs* transcription were not significantly altered. Hence, furanone appeared to alter AI-2 signaling post-transcriptionally. © 2004 Wiley Periodicals, Inc.

Keywords: furanone; AI-2; quorum sensing antagonist

Correspondence to: Thomas K. Wood

*Present address: School of Chemical and Biomolecular Engineering, Cornell University, Ithaca, NY

INTRODUCTION

It is generally accepted that bacteria use quorum sensing to control some gene expression by sensing their population through small signaling compounds called autoinducers (AI) that are secreted into the environment (Bassler, 1999). As the AI concentration increases with cell density, the binding of AIs to the cellular receptors will trigger downstream genes for different phenotypes including bioluminescence (Cao and Meighen, 1989), production of virulence factors (Beck von Bodman et al., 1998), siderophore synthesis (Stintzi et al., 1998), protein production (DeLisa et al., 2001a), biofilm formation (Davies et al., 1998), and plasmid conjugation (Lithgow et al., 2001). Controlling gene expression at an appropriate cell density has advantages for bacteria; for example, if the bacteria express virulence factors at very low cell densities, the cells risk alerting the host too early and may be more readily killed by the immune response (Bassler, 1999). Hence, the quorum sensing system triggers specific processes only when the cell density is high to ensure these phenotypes are productive (Xavier and Bassler, 2003).

Different species use different quorum sensing signals, and AIs are mainly divided into two groups, acylated homoserine lactones (AHL or AI-1, regulated by LuxI/LuxR-type systems) for Gram-negative bacteria and peptides for Gram-positive bacteria (Bassler, 1999). Interestingly, signal AI-2 (produced by LuxS) is a species non-specific signal, existing in both Gram-negative and Gram-positive bacteria (Surette et al., 1999). Due to its common role in quorum sensing, AI-2 has been the subject of much research recently. AI-2 exists in many different species, e.g., 35 of the 89 fully sequenced bacterial strains have the *luxS* gene (Xavier and Bassler, 2003); however, the roles of *luxS*

in bacteria are not clear. Recent studies have suggested AI-2 regulates virulence factors (Fong et al., 2001; Sperandio et al., 2001), an ABC transport system (Taga et al., 2001), light production (Lilley and Bassler, 2000), motility (Sperandio et al., 2001), and biofilm formation (McNab et al., 2003).

The central metabolite S-adenosylmethionine (SAM) is used as a precursor in both the AI-2 and AHL pathways (Xavier and Bassler, 2003). SAM is processed by LuxI-like enzymes to produce AHL along with a toxic byproduct, methylthioadenosine, which is then transformed to non-toxic methylthioribose by 5′methylthioadenosine/S-adenosylhomocysteine nucleosidase (Pfs). In the AI-2 synthetic pathway, SAM is converted to S-adenosylhomocysteine (SAH) by a methyltransferase, SAH is converted to S-ribosylhomocysteine (SRH) by Pfs, and SRH is converted to 4,5-dihydroxy 2,3-pentanedione by LuxS, which then appears to form the active AI-2 molecule as a furanosyl borate diester (Chen et al., 2002). Similar to the AHL pathway, the AI-2 synthetic pathway also produces a toxic intermediate, SAH, which is detoxified by either Pfs or SAH hydrolase (Xavier and Bassler, 2003).

Since quorum sensing regulates a broad spectrum of bacterial phenotypes, it is intriguing to try to control deleterious bacterial multicellular behavior by inhibiting the quorum sensing system. Recently, several brominated furanones have been isolated from the surface of the marine red alga *Delisea pulchra* and have been shown to inhibit some multicellular behavior of Gram-negative bacteria such as swarming (Gram et al., 1996; Ren et al., 2001), bioluminescence (Manefield et al., 2000), and biofilm formation (Hentzer et al., 2002; Ren et al., 2001) without affecting general growth. Also, it has been demonstrated that furanones inhibit cell communication based on AI-1 (Manefield et al., 1999) and AI-2 (Ren et al., 2001). By using 2D-PAGE for *E coli* harboring the bioluminescent genes *luxR* and *luxCDABE*, Manefield et al. (1999) found 4-bromo-5-(bromomethylene)-3-(1-hydroxybutyl)-2(*5H*)-furanone upregulated six proteins (Zwf, AhpC, and four unknown proteins) and down-regulated six proteins (LuxA, LuxB, LuxD, OmpF, DnaK, and GlnA). Also, it was reported that furanone could increase the turnover of LuxR (Manefield et al., 2002). Hence, the instability of LuxR appears to explain the interference of furanone with AI-1. Recently, Hentzer et al. (2003) found by using DNA microarrays that the synthetic 4-bromo-5-(bromomethylene)-2(*5H*)-furanone (henceforth synthetic furanone) repressed 85 genes of *Pseudomonas aeruginosa* PAO1, 80% of which are also induced by AI-1 quorum sensing. Compared to the well-documented studies about furanone inhibition of AI-1 quorum sensing, the mechanism of furanone inhibition of AI-2 signaling on a genetic basis is poorly understood, and in the present study, DNA microarrays were used to compare whole-genome gene expression of *E. coli* cells with and without furanone.

DNA microarrays have been used to monitor global gene expression profiles in response to different stimuli (Shoemaker and Linsley, 2002) including heat shock and other stresses (Helmann et al., 2001; Wilson et al., 1999; Zheng et al., 2001), quorum sensing (DeLisa et al., 2001b; Sperandio et al., 2001), anaerobic metabolism (Ye et al., 2000), sporulation (Fawcett et al., 2000), and biofilm formation (Ren et al., 2003, 2004; Schembri et al., 2003; Stanley et al., 2003; Whiteley et al., 2001). Sperandio et al. (2001) used DNA microarrays to study gene expression of wild-type and LuxS mutant *E. coli* O157:H7 strains, and found that AI-2 is a global regulatory signal which regulates more than 400 genes. The up-regulated genes include those for chemotaxis, flagella synthesis, motility, and virulence factors. DeLisa et al. (2001b) did a similar experiment to study the gene expression of a *luxS* mutant of *E. coli* K12 derivative W3110 contacted with AI-2^+ or AI-2^- supernatant; however, their results were significantly different from that of Sperandio et al. The present study is an effort to discern how both AI-2 and furanone function; DNA microarrays were used in the present study to compare both the gene expression profile of AI-2^+ wild-type strain *E. coli* K12 and AI-2^- mutant DH5α (Surette and Bassler, 1998) as well as compare the gene expression profiles with and without furanone. One hundred and forty-three new AI-2-controlled genes were discovered (91 with known functions and 52 with unknown functions), and 90 new genes were identified whose expression is influenced by the presence of furanone (62 with known functions and 28 with unknown functions). This is the first report about the genetic basis of the inhibition of furanone on AI-2 signaling.

MATERIALS AND METHODS

Bacterial Strains and Growth Media

Escherichia coli DH5α [*luxS supE*44 Δ*lacU*169 (ϕ80 *lacZ*ΔM15) *hsdR*17 *recA*1 *endA*1 *gyrA*96 *thi*-1 *relA*1] and *E. coli* K12 wild-type (ATCC 25404) were used as AI-2^- and AI-2^+ strains, respectively. *E. coli* DH5α lacks AI-2 activity due to a 60 amino acid truncation stemming from a one bp deletion that results in early truncation of *luxS* (formerly *ygaG*) (Surette et al., 1999). *E. coli* JM109 (*recA*1 *supE*44 *endA*1 *hsdR*17 *gyrA*96 *relA1 thi* Δ(*lac-proAB*) F′[*traD*36 *proAB*$^+$ *lacI*^{q} *lacZ*ΔM15]) was used to study the formation of the air−liquid interface biofilm. LB medium (Sambrook et al., 1989) containing 10 g/L tryptone, 5 g/L yeast extract, and 10 g/L NaCl and supplemented with 0.5% glucose was used to grow the strains for RNA isolation and for preparing the *E. coli* supernatant for the AI-2 bioassay. The quorum-sensing mutant strain of *Vibrio harveyi*, BB170 (sensor 1^-, sensor 2^+), was obtained from Dr. B. Bassler (Surette and Bassler, 1998). Autoinducer bioassay (AB) medium (Greenberg et al., 1979) was used to grow *V. harveyi* BB170, and LM medium (Bassler et al., 1994) was used to determine the *V. harveyi* colony forming units (CFU).

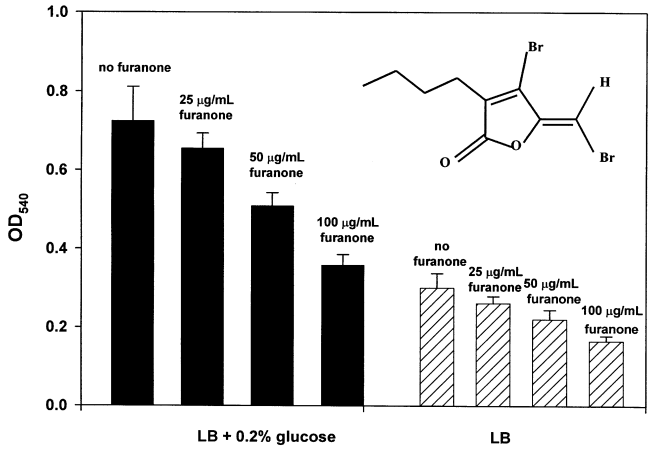

Figure 1. Inhibition of the formation of the *E. coli* air–liquid interface biofilm by addition of 25–100 μg/mL furanone. Data are from 48-h biofilms. The structure of (*5Z*)-4-bromo-5-(bromomethylene)-3-butyl-2(*5H*)-furanone is shown in the top right-corner.

Furanone Preparation

(*5Z*)-4-Bromo-5-(bromomethylene)-3-butyl-2(*5H*)-furanone (Fig. 1) was synthesized as described previously (Beechan and Sims, 1979; Manny et al., 1997; Ren and Wood, 2004). The furanone was dissolved in 95% ethanol to 14.9 mg/mL and stored at 4°C.

Total RNA Isolation for DNA Microarrays

To identify the genes controlled by AI-2, *E. coli* DH5α and K12 were grown overnight in LB, diluted 1:100 in fresh LB supplemented with 0.5% glucose, and grown to an optical density at 600 nm (OD) of 0.9. The cells were harvested by centrifuging for 15 s at 20,000*g* in cold (−80°C) mini bead beater tubes (Biospec, Bartlesville, OK) in a microcentrifuge. The cell pellets were flash frozen in a dry ice–ethanol bath and stored at −80°C until RNA isolation. To study the gene expression affected by furanone, *E. coli* K12 cells were grown overnight in LB, diluted 1:100 in fresh LB supplemented with 0.5% glucose and 0 or 60 μg/mL furanone (same amount of solvent, 0.67%, was added to both samples to eliminate solvent effects), and grown to OD = 0.9. The cells were harvested for RNA in the same way as in the AI-2 experiment.

To lyse the cells, 1.0 mL RLT buffer (Qiagen, Inc., Valencia, CA) and 0.2 mL 0.1 mm zirconia/silica beads (Biospec) were added to the frozen bead beater tubes containing the cell pellets. The tubes were closed tightly and beat for 30 s at the maximum speed in a mini bead beater (Cat. No. 3110BX, Biospec). The total RNA was isolated by following the protocol of the RNeasy Mini Kit (Qiagen) including an on-column DNase digestion with RNase-free DNase I (Qiagen). An OD (optical density) reading at 260 nm was used to quantify the RNA yield. OD_{260}/OD_{280} and 23S/16S rRNA were measured to check the purity and integrity of RNA (RNeasy Mini handbook, Qiagen).

DNA Microarrays

The *E. coli* DNA microarrays were prepared as described previously (Wei et al., 2001). Each gene probe was synthesized by PCR and has a size of the full open reading frame (200–2000 nt). The double-stranded PCR products were denatured in 50% dimethyl sulfoxide and spotted onto aminosilane slides (Full Moon Biosystems, Sunnyvale, CA) as probes to hybridize with the mRNA-derived cDNA samples. It has been shown that each array can detect 4228 of the 4290 *E. coli* ORFs (Wei et al., 2001). Each gene has two spots per slide.

Synthesis of Cy3- or Cy5-Labeled cDNA

To convert the total RNA into labeled cDNA, reverse transcription was performed in 1.5 mL microcentrifuge tubes (Fisher) to which 6 μg of total RNA and 6 μg of random hexamer primers (Invitrogen Corp., Carlsbad, CA) were added, and the volume was adjusted to 24 μL with RNase-free water (Invitrogen). The mixture was incubated 10 min at 70°C followed by 10 min at room temperature for annealing, then the reaction components were added consisting of 8 μL 5× SuperScript II reaction buffer (Invitrogen), 4 μL 0.1*M* dithiothreitol (DTT) (Invitrogen), 1 μL of a deoxynucleoside triphosphates (dNTPs) mix (2 m*M* each of dATP, dGTP, dTTP and 1 m*M* dCTP), 1 μL 0.5 m*M* Cy3- or Cy5-labeled dCTP (Amersham Biosciences, Piscataway, NJ), and 2 μL SuperScript II reverse transcriptase (10 U/μL, Invitrogen). cDNA synthesis was conducted at 42°C for 2 h and stopped by heating at 94°C for 5 min. After cDNA synthesis, the RNA template was removed with 2 μL 2.5*M* NaOH. The pH was neutralized with 10 μL 2*M* HEPES buffer, and the cDNA was purified with a Qiaquick PCR Mini Kit (Qiagen). The efficiency of labeling was checked via absorbance at 260 nm for the cDNA concentration, at 550 nm for Cy3 incorporation, and at 650 nm for Cy5 incorporation.

Hybridization and Washing

The *E. coli* K12 and DH5α suspension cDNA samples (6 μg of each) were each labeled with both Cy3 and Cy5 dyes to remove artifacts related to different labeling efficiencies; hence, each experiment required at least two slides. The Cy3-labeled *E. coli* K12 sample and Cy5-labeled *E. coli* DH5α sample were hybridized on the first slide. Similarly, the Cy5-labeled *E. coli* K12 sample and Cy3-labeled *E. coli* DH5α sample were hybridized on the second slide. Since each gene has two spots on a slide, the two hybridizations generated 8 data points for each gene (4 points for the *E. coli* K12 sample and 4 points for the DH5α sample). DNA microarrays for the *E. coli* K12 cDNA samples with and without furanone were performed in an analogous manner.

The DNA microarrays were incubated in prehybridization solution [3.5X SSC (Invitrogen), 0.1% SDS (Invitrogen), 0.1% bovine serum albumin (Invitrogen)] at 45°C for

Table I. *Escherichia coli* genes induced by AI-2 or repressed by furanone (genes in boldface were changed by both compounds). P_v is *p*-value.

Gene	b#	Function of the product	AI-2 affected fold change	Furanone affected fold change
Chemotaxis and aerotaxis				
aer	b3072	Aerotaxis sensor receptor, flavoprotein	5.3	−4.6
cheA	b1888	Enzyme, chemotaxis, and mobility; sensory transducer kinase between chemo- signal receptors and CheB and CheY	13.7	−22.9
cheB	b1883	Response regulator for chemotaxis (cheA sensor), protein methylesterase	5.7	−7.7
cheR	b1884	Response regulator for chemotaxis, protein glutamate methyltransferase	2.9	−4.8
cheW	b1887	Positive regulator of CheA protein activity	4.7	−13.7
cheY	b1882	Chemotaxis regulator transmits chemoreceptor signals to flagellar motor components	3.2	−4.5
cheZ	b1881	Chemotactic response, CheY protein phophatase, antagonist of CheY as switch regulator	9.0	−6.5
tap	b1885	Regulator, chemotaxis and mobility methyl-accepting chemotaxis protein IV, peptide sensor receptor	10.2	−312
tar	b1886	Regulator, chemotaxis and, mobility; methyl-accepting chemotaxis protein II, aspartate sensor receptor	22.5	−13.3
tsr	b4355	Methyl-accepting chemotaxis protein I, serine sensor receptor	28.4	−18.1
trg	b1421	Regulator, chemotaxis, and motility	2.6	−2.4
Flagellar biosynthesis			(P_v = 0.44)	
flgA	b1072	Flagellar biosynthesis, assembly of basal-body periplasmic P ring	4.0	−4.8
flgB	b1073	Flagellar biosynthesis, cell-proximal portion of basal-body rod	7.7	−8.2
flgC	b1074	Flagellar biosynthesis, cell-proximal portion of basal-body rod	10.0	−12.4
flgD	b1075	Flagellar biosynthesis, initiation of hook assembly	6.9	−10.6
flgE	b1076	Flagellar biosynthesis, hook protein	7.7	−10.6
flgF	b1077	Flagellar biosynthesis, cell-proximal portion of basal-body rod	6.8	−6.9
flgG	b1078	Flagellar biosynthesis, cell-distal portion of basal-body rod	7.6	−9.3
flgH	b1079	Flagellar biosynthesis, basal-body outer-membrane L (lipopolysaccharide layer) ring protein	4.9	−8.2
flgI	b1080	Homolog of Salmonella P-ring of flagella basal body	3.1	−4.1
flgJ	b1081	Flagellar biosynthesis	3.3	−2.9
flgK	b1082	Flagellar biosynthesis, hook-filament junction protein 1	11.6	−8.8
flgL	b1083	Flagellar biosynthesis, hook-filament junction protein	3.5	−9.3
flgM	b1071	Anti-FliA (anti-sigma) factor, also known as Rf1B protein	4.5	−6.0
flgN	b1070	Protein of flagellar biosynthesis	3.8	−3.5
fliA	b1922	Flagellar biosynthesis, alternative sigma factor 28, regulation of flagellar operons	2.6	−2.0
fliC	b1923	Flagellar biosynthesis, flagellin, filament structural protein	17.2	−26.3
fliD	b1924	Flagellar biosynthesis, filament capping protein, enables filament assembly	13.2	−8.3
fliF	b1938	Flagellar biosynthesis, basal-body MS (membrane and supramembrane)-ring and collar protein	7.4	−8.6
fliH	b1940	Flagellar biosynthesis, export of flagellar proteins?	7.8	−5.3
fliI	b1941	Flagellum-specific ATP synthase	4.2	−5.9
fliK	b1943	Flagellar hook-length control protein	3.4	−3.7
fliL	b1944	Flagellar biosynthesis	2.3	−2.5
fliM	b1945	Flagellar biosynthesis, component of motor switch and energizing, enabling rotation and determining its direction	1.8	−2.0
fliN	b1946	Flagellar biosynthesis, component of motor switch and energizing, enabling rotation and determining its direction	28.3	−30
fliO	b1947	Flagellar biosynthesis	2.7	−3.0
fliP	b1948	Flagellar biosynthesis	3.8	−3.3
fliQ	b1949	Flagellar biosynthesis	4.8	−2.2
motA	b1890	Proton conductor component of motor, no effect on switching	5.1	−10.4
motB	b1889	Enables flagellar motor rotation, linking torque machinery to cell wall	5.1	−7.8
Genes with other functions and unknown genes				
b1044	b1044	Orf, unknown	2.2	−2.4
b0298	b0298	Putative factor, not classified	2.9	−1.3
b0329	b0329	Orf, unknown	3.0	1.5
b0373	b0373	Putative factor, not classified	3.0	−1.2
b1194	b1194	Orf, hypothetical protein	6.3	−4.0
b1436	b1436	Orf, unknown	3.5	2.2
b1566	b1566	Orf, hypothetical protein, also known as *flaX*	8.8	−7.1
b1729	b1729	Putative enzyme, not classified	3.3	1.5
b1760	b1760	Orf, unknown	4.9	−2.4
b1880	b1880	Structural component, not classified	3.0	−3.5
b1936	b1936	Orf, hypothetical protein	2.2	−3.8
b2973	b2973	Orf, unknown	−0.8	−2.4
b2974	b2974	Putative structure, not classified	1.3	−2.5

Table I. Continued

Gene	b#	Function of the product	AI-2 affected fold change	Furanone affected fold change
b3524	b3524	Orf, unknown	1.2	−2.2
fliY	b1920	Putative periplasmic binding transport protein	1.9	−3.5
b2256	b2256	Orf, unknown	3.2	1.3
b2442	b2442	IS, phage, Tn, not classified	3.5	1.4
cysJ	b2764	Enzyme, central intermediary metabolism: sulfur metabolism	2.6	1.2
fliZ	b1921	Orf, hypothetical protein, function unknown	10.5	−9.3
frvR	b3897	Putative regulator, not clasified	3.1	1.7
gatC	b2092	Transport, transport of small molecules: carbohydrates, organic acids, alcohols	6.6	−1.2
gatR_2	b2090	Galactitol utilization operon repressor	2.7	2.7
lacA	b0342	Thiogalactoside acetyltransferase	3.3	−1.1
lacY	b0343	Galactoside permease (M protein)	18.7	−1.3
lacZ	b0344	Beta-D-galactosidase	15.4	−1.1
malE	b4034	Transport, transport of small molecules: carbohydrates, organic acids, alcohols	1.4	−2.3
mglB	b2150	Galactose-binding transport protein, receptor for galactose taxis	3.7	−1.0
oppA	b1243	Transport, protein, peptide secretion	3.2	1.1
oppC	b1245	Putative transport, not classified	2.5	−1.0
phnI	b4099	Phosphonate metabolism	4.1	−5.8
phoA	b0383	Enzyme, central intermediary metabolism: phosphorous compounds	2.7	1.1
pta	b2297	Enzyme, degradation of small molecules: carbon compounds	2.8	1.0
ptsP	b2829	PTS system, enzyme I, transcriptional regulator	1.4	−3.1
rbsB	b3751	D-ribose, periplasmic binding protein	2.7	2.3
tehA	b1429	Transport, drug/analog sensitivity	1.4	−2.6
trkH	b3849	Transport, transport of small molecules: cations	5.5	2.7
yeeD	b2012	Orf, unknown	2.7	1.3
yeeE	b2013	Putative transport, not classified	3.2	1.1
yhjH	b3525	Orf, hypothetical protein	6.0	−9.9

20 min. The arrays were rinsed with double-distilled water (ddH_2O) and spun dry by centrifugation. Labeled cDNA (6 μg) was concentrated to 10 μL total volume and mixed with 10 μL 4X cDNA hybridization solution (Full Moon Biosystems) and 20 μL formamide (EM Science, Gibbstown, NJ). The hybridization mix was heated to 95°C for 2 min and added to the DNA microarrays; each array was covered with a coverslip (Corning, Big Flats, NY) and incubated overnight at 37°C for hybridization. When the hybridization was finished, the coverslips were removed in 1X SSC, 0.1% SDS at room temperature, and the arrays were washed once for 5 min in 1X SSC, 0.1% SDS at 40°C, twice for 10 min in 0.1X SSC, 0.1% SDS at 40°C, and twice for 1 min in 0.1X SSC at 40°C. The arrays were quickly rinsed by dipping in room temperature ddH_2O and then spun dry by centrifugation.

Image and Data Analysis

The hybridized slides were scanned with the Generation III Array Scanner (Molecular Dynamics Corp.). Scans used 570 nm and 670 nm to quantify the probes labeled with Cy3 and Cy5 separately. The signal was quantified with Array Vision 4.0- or 6.0-version software (Imaging Research, Ontario, Canada). Genes were identified as differentially expressed if the expression ratio was greater than 2.5 (for the AI-2 experiments) or 2 (for the furanone experiments) based on one standard deviation and based on a *p*-value (*t*-test) less than 0.05. *P*-values were calculated on log-transformed, normalized intensities. Including the *p*-value criterion ensures the reliability of the induced/repressed gene list. Normalization was relative to the median total fluorescent intensity per slide per channel. The gene functions were obtained from the database in National Center for Biotechnology Information (http://www.ncbi.nlm.nih.gov/).

RNA Dot Blotting

Digoxigenin (DIG)-labeled DNA probes of six genes, *flgC*, *fliC*, *b1194*, *b1566*, *yhjH*, and *cheA*, were synthesized using the PCR DIG Probe Synthesis Kit (Roche Applied Science, Mannheim, Germany). The PCR was performed in 30 cycles at 95°C for 30 s, 60°C for 30 s, and 72°C for 40 s. The final extension was at 72°C for 7 min. The probes have lengths of 400 bp except for *flgC* (328 bp) and *b1566* (285 bp) due to the size of the genes (see Table IV for specific primers). Total RNA (1.25, 2.5, or 5 μg) from independent cell cultures (different experiments than those used for the DNA microarrays but identical culture conditions of K12 vs. DH5α as well as K12 with and without 60 μg/mL furanone) was blotted on positively charged nylon membranes (Boehringer Ingelheim, Ridgefield, CT) using a Bio-Dot Microfiltration Apparatus (Bio-Rad,

Table II. *Escherichia coli* genes repressed by AI-2 (highlighted genes were also induced by furanone).

Gene	b#	Function of the product	Fold change
agaY	b3137	Enzyme, central intermediary metabolism: pool, multipurpose conversions	−4.7
appA	b0980	Enzyme, central intermediary metabolism: pool, multipurpose conversions	−3.5
araE	b2841	Transport, transport of small molecules: carbohydrates, organic acids, alcohols	−3.0
aslB	b3800	Regulator, not classified	−2.7
asnA	b3744	Enzyme, amino acid biosynthesis: asparagine	−2.7
asnC	b3743	Regulator, amino acid biosynthesis: asparagine	−19
b0352	b0352	Enzyme, degradation of small molecules: carbon compounds	−4.5
b0487	b0487	Putative transport, not classified	−3.0
b0617	b0617	Enzyme, central intermediary metabolism: pool, multipurpose conversions	−2.5
b1145	b1145	Putative phage repressor	−11.9
b1164	b1164	Orf, hypothetical protein	−2.6
b1165	b1165	Orf, hypothetical protein	−2.8
b1166	b1166	Orf, hypothetical protein	−3.4
b2464	b2464	Enzyme, central intermediary metabolism: non-oxidative branch, pentose pathway	−3.0
b2875	b2875	Putative enzyme, not classified	−3.8
b2884	b2884	Orf, hypothetical protein	2.7
b2950	b2950	Putative transport, not classified	−3.1
b3024	b3024	Orf, hypothetical protein	−5.8
b3100	b3100	Orf, hypothetical protein	−6.1
b3515	b3515	Putative regulator, not classified	−3.3
b3592	b3592	Putative enzyme, not classified	−4.2
b3698	b3698	Orf, hypothetical protein	−6.7
cirA	b2155	Outer membrane receptor for iron-regulated colicin I receptor, porin, requires *tonB* gene product	−5.7
crr	b2417	Enzyme, transport of small molecules: carbohydrates, organic acids, alcohols	−2.6
cvpA	b2313	Membrane protein required for colicin V product	−3.0
cysA	b2422	Transport, transport of small molecules: anions	−3.5
dps	b0812	Global regulator, starvation conditions	−3.2
eda	b1850	Enzyme, central intermediary metabolism: Entner-Douderoff	−3.3
entB	b0595	Enzyme, biosynthesis of cofactors, carriers: Enterochelin	−6.1
entE	b0594	Enzyme, biosynthesis of cofactors, carriers: Enterochelin	−2.6
fpr	b3924	Enzyme, central intermediary metabolism: pool, multipurpose conversions	−3.4
gadA	b3517	Enzyme, central intermediary metabolism: pool, multipurpose conversions	−6.8
gadB	b1493	Enzyme, central intermediary metabolism: pool, multipurpose conversions	−12.2
glcD	b2979	Enzyme, degradation of small molecules: carbon compounds	−2.6
gldA	b3945	Enzyme, central intermediary metabolism: pool, multipurpose conversions	−2.6
gltA	b0720	Enzyme, energy metabolism, carbon: TCA cycle	−2.6
gltF	b3214	Regulator, central intermediary metabolism: pool, multipurpose conversions	−5.5
glyA	b2551	Enzyme, amino acid biosynthesis: glycine	−5.0
hdeA	b3510	Orf, hypothetical protein	−13.2
hdeB	b3509	Orf, hypothetical protein	−17.8
hdeD	b3511	Orf, hypothetical protein	−5.7
hslS	b3686	Heat shock protein	−8.5
ilvI	b0077	Acetolactate synthase isozyme III large subunit	−2.6
insA_1	b0022	IS, phage, Tn, transposon-related functions	−3.3
insA_2	b0265	IS, phage, Tn, transposon-related functions	−4.4
insA_3	b0275	IS, phage, Tn, transposon-related functions	−4.1
insA_5	b1894	IS, phage, Tn, transposon-related functions	−2.7
insB_3	b0274	IS, phage, Tn, transposon-related functions	−3.0
katE	b1732	Enzyme, detoxification	−2.7
kdgK	b3526	Enzyme, degradation of small molecules: carbon compounds	−5.4
kduD	b2842	Enzyme, central intermediary metabolism: pool, multipurpose conversions	−29
kduI	b2843	Enzyme, degradation of small molecules: carbon compounds	−30
metF	b3941	Enzyme, central intermediary metabolism: pool, multipurpose conversions	−2.6
osmY	b4376	Hyperosmotically inducible periplasmic protein	−2.9
otsA	b1896	Enzyme osmotic adaptation	−2.5
otsB	b1897	Enzyme osmotic adaptation	−2.6
panF	b3258	Transport, transport of small molecules: cations	−3.1
pheA	b2599	Enzyme, amino acid biosynthesis: phenylalanine	−12.2
poxB	b0871	Enzyme, degradation of small molecules: carbon compounds	−3.1
ptsH	b2415	Enzyme, transport of small molecules: carbohydrates, organic acids, alcohols	−6.0
ptsI	b2416	Enzyme, transport of small molecules: carbohydrates, organic acids, alcohols	−7.0
ptsN	b3204	Enzyme, transport of small molecules: amino acids, amines	−2.5
purD	b4005	Enzyme, purine ribonucleotide biosynthesis	−8.7
purE	b0523	Enzyme, purine ribonucleotide biosynthesis	−3.6

Table II. Continued

Gene	b#	Function of the product	Fold change
purF	b2312	Enzyme, purine ribonucleotide biosynthesis	−3.6
purH	b4006	Enzyme, purine ribonucleotide biosynthesis	−8.5
purK	b0522	Enzyme, purine ribonucleotide biosynthesis	−4.3
purM	b2499	Enzyme, purine ribonucleotide biosynthesis	−6.0
purT	b1849	Enzyme, purine ribonucleotide biosynthesis	−5.1
slp	b3506	Membrane, outer membrane constituents	−6.5
sodA	b3908	Enzyme, detoxification	−2.8
soxS	b4062	Regulation of superoxide response regulon	−3.1
sucC	b0728	Enzyme, energy metabolism, carbon: TCA cycle	−2.5
sucD	b0729	Enzyme, energy metabolism, carbon: TCA cycle	−3.4
tesB	b0452	Enzyme, fatty acid and phosphatidic acid biosynthesis	−387
tyrP	b1907	Transport, transport of small molecules: amino acids, amines	−3.5
ugpB	b3453	Transport, transport of small molecules: carbohydrates, organic acids, alcohols	−2.8
ugpQ	b3449	Enzyme, central intermediary metabolism: pool, multipurpose conversions	−3.3
xasA	b1492	Putative transport, not classified	−12
ybaC	b0476	Orf, not classified	−2.7
ycdB	b1019	Orf, hypothetical protein	−2.6
ydhC	b1660	Putative transport, not classified	−2.9
ygaE	b2664	Putative regulator, not classified	−2.7
yhaQ	b3112	Putative enzyme, not classified	−2.6
yhhS	b3473	Putative transport, not classified	−2.7
yhiD	b3508	Putative transport, not classified	−7.1
yhiU	b3513	Putative membrane, not classified	−9.2
yhiX	b3516	Putative regulator, not classified	−6.3
yhjL	b3530	Putative enzyme, not classified	−7.5
yhjM	b3531	Putative enzyme, not classified	−4.2
yhjN	b3532	Orf, unknown	−5.0
yiaJ	b3574	Putative regulator, not classified	−3.0
yicE	b3654	Putative transport, not classified	−9.7
yigB	b3812	Putative enzyme, not classified	−3.1
yigJ	b3823	Orf, unknown	−3.3
yjbQ	b4056	Orf, unknown	−3.2
yjcD	b4064	Orf, unknown	−3.6
yjgK	b4252	Orf, unknown	−6.1
yqjE	b3099	Orf, unknown	−2.8

Richmond, CA). Total RNA was fixed by baking for 2 h at 80°C. DNA probes (about 400 ng, a serial dilution of RNA samples was tested to ensure excess of the DNA probes) were denatured in boiling water for 5 min before hybridizing to RNA. Hybridization (50°C, 16 h) and washing were conducted by following the protocol for DIG labeling and detection (Roche Applied Science). To detect the signal, disodium 3-(4-methoxyspiro {1,2-dioxetane-3,2-(5-chloro)tricycle [3.3.1.1,7] decan}-4-yl) phenyl phosphate (Roche Applied Science) was used as a substrate to give chemiluminescence, and the light was recorded by Biomax X-ray film (Kodak, Rochester, NY).

Autoinducer Activity Assay

Bacterial supernatants were assayed using the method of Surette and Bassler (1998) as described previously. Briefly, *E. coli* DH5α and K12 were grown overnight in LB medium containing 0.5% glucose and diluted 1:100 in the same fresh medium. When the cell density reached an optical density at 600 nm (OD) of 0.9, it was centrifuged at 13,800*g* for 10 min at 4°C. The supernatant was then passed through a 0.2 μm cellulose nitrate membrane filter (Whatman, Maidstone, England). The cell−free supernatant was stored at −20°C.

The reporter strain *V. harveyi* BB170 was grown in AB medium overnight, diluted 1:5000 into the fresh AB medium, then the cell-free supernatants from the *E. coli* samples were added at a concentration of 10% (v/v). The time course of bioluminescence was measured with a 20/20 luminometer (Turner Design, Sunnyvale, CA) and reported as relative light units. The cell density of the *V. harveyi* reporter strain was measured by spreading the cells on LM plates and counting colony forming units (CFU) after 24 h. Each experiment was conducted in duplicate.

96-Well Plate Assay of Biofilm Formation

This assay was adapted from reported protocols (Li et al., 2001; Pratt and Kolter, 1998). *E. coli* JM109 was grown in LB medium supplemented with or without additional glucose and different concentrations of furanone in polystyrene 96-well plates at 37°C for 2 days without shaking. The same amount of 95% ethanol was added to each well

to eliminate the effect of solvent. Four identical 96-well plates were prepared, and one plate was processed every 16–24 h to get a time course of biofilm formation (at the air–liquid interface). To quantify the biofilm mass, the cell suspension was removed, and the plates were washed 3 times with water. The biofilms were stained with 0.1% crystal violet for 20 min, and the extra dye was removed by washing 3 times with water. The remaining dye (staining the biofilms) was dissolved with 300 μL 95% ethanol, and the OD reading at 620 nm was measured to quantify the biofilm mass. Each data point was averaged from six replicate wells and the standard deviations were calculated.

RESULTS

Genes for Chemotaxis, Flagella, and Motility are Induced by AI-2

In the present study, *E. coli* K12 was found to have AI-2 activity 620 times higher than the AI-2 negative strain *E. coli* DH5α (Surette and Bassler, 1998) based on the AI-2 assay with *V. harveyi* BB170 (1.3×10^{-4} light units vs. 2.1×10^{-7} light units). Therefore, *E. coli* K12 was used as the AI-2-positive strain and compared with *E. coli* DH5α in the first set of DNA microarray studies, which were used to determine the genes controlled by AI-2. It was found that AI-2 regulated 166 genes; 67 were induced more than 2.5-fold (Table I) and 99 were repressed more than 2.5-fold (Table II). Genes in the same operons were found induced together (e.g., of the 53 induced genes with known functions, 7 operons were induced including *flgABCDEFGHIJKLMN*, which were induced 3.5–10-fold) or repressed together (e.g., of the 62 repressed genes with known functions, 10 operons were repressed including *purDEFHKMT*, which were repressed 3.6–8.7-fold), indicating that the RNA was of good quality and the hybridizations were successful. Among the up-regulated genes, most of them are for chemotaxis, flagella synthesis, and motility, such as *cheA* (14-fold), *tap* (10-fold), *flgC* (10-fold), and *fliN* (28-fold). These results agreed with the previous study of Sperandio et al. (2001), which reported that chemotaxis, flagella, and motility genes were induced by AI-2, e.g., *cheA* was induced by fourfold. Interestingly, 14 of the 67 genes induced here by AI-2 have unknown functions, such as *b1566* (induced 10-fold, Table I). There were 44 newly discovered AI-2-induced genes (30 with known functions and 14 with unknown functions) different from the two previous reports (DeLisa et al., 2001b; Sperandio et al., 2001).

Genes Repressed by AI-2

In the present study, 99 genes were repressed in *E. coli* K12 compared to *E. coli* DH5α, therefore these genes may be repressed by AI-2 (Table II). Most of these genes belong to the functional groups of central intermediary metabolism (10 genes, such as *agaY*, *appA*, *b0617*, *fpr*, and *gadAB*), biosynthesis (such as *asnA*, *glyA*, and *purDEFHKMT*), transposons (*insA_12345*), and 38 genes with unknown functions.

Genes for Chemotaxis, Flagella, and Motility are Repressed by Furanone

Previously, we have shown that 5–10 μg/mL furanone inhibited quorum sensing via AI-2 of *V. harveyi* 132-fold to 5500-fold as well as inhibited the quorum sensing of *E. coli* via AI-2 379–26,600 fold (Ren et al., 2001). To identify which genes were controlled by furanone and to investigate whether furanone inhibited quorum sensing by inhibiting the same genes affected by AI-2, DNA microarrays were used to compare the gene expression profiles of *E. coli* K12 with and without 60 μg/mL furanone. There was no effect of furanone on growth rate at this concentration (1.91 h^{-1} without furanone vs. 1.83 h^{-1} with 60 μg/mL furanone). Genes in the same operon were found induced together (such as *hdeABD* were induced 2.3–3.9-fold) or repressed together (of the 56 repressed known genes, 4 operons were repressed including *flgABCDEFGHIJKLMN*, which were repressed 3.5–12-fold), indicating that the RNA isolation and hybridizations were of good quality (see Table I for a comparison of the two data sets). Furanone induced 34 genes (Table III) and repressed 56 genes (Table I) greater than twofold. The 90 genes differentially expressed by furanone constitute 2.1% of the total 4228 genes detectable by the DNA microarrays.

Interestingly, 39 of the 56 repressed genes (70%) were related to chemotaxis, flagella synthesis, and motility, such as *cheR* (4.8-fold), *flgA* (4.8-fold), *fliC* (26.3-fold), and *motA* (10.4-fold). The genes repressed by furanone (56 genes) overlapped with those induced by AI-2 (67 genes) as 79% (44 genes) of the genes repressed by furanone are those induced by AI-2 (Table I). Therefore, the microarray results support that furanone inhibited phenotypes like biofilm formation (discussed below) by interrupting the same suite of genes controlled by AI-2. Interestingly, *luxS* and *pfs* (genes required for AI-2 signal synthesis; Schauder et al., 2001) were neither induced nor repressed (data not shown). DeLisa et al. (2001b) showed that neither of these genes was controlled by AI-2, and here we show that the expression of these two genes are also not subject to regulation by furanone.

Genes Induced by Furanone

Sixty-five percent (22 out of 34) of the genes induced by furanone have uncharacterized functions. Although 79% of the genes repressed by furanone are those induced by AI-2 (44 genes, Table I), only eight of the genes induced by furanone were repressed by AI-2 (*asnA*, *b1165*, *gadB*, *hdeABD*, *ugpB*, and *yhiX*). These genes are involved in asparagine synthesis (*asnA*), central intermediary metab-

Table III. *Escherichia coli* genes induced by 60 μg/mL of furanone (highlighted genes were also repressed by AI-2).

Gene	b#	Function of product	Fold change
asnA	b3744	Enzyme, amino acid biosynthesis: asparagine	2.9
b0220	b0220	Orf, hypothetical protein	2.1
b0753	b0753	Putative regulator, not classified	2.6
b0987	b0987	Orf, unknown	2.2
b1165	b1165	Orf, unknown	2.1
b1171	b1171	Orf, unknown	2.2
b1172	b1172	Orf, unknown	2.2
b1650	b1650	Enzyme, central intermediary metabolism: pool, multipurpose conversions	4.3
b2670	b2670	Orf, unknown	2.1
b2772	b2772	Orf, unknown	2.5
b3023	b3023	Orf, unknown	4.6
bioB	b0775	Enzyme, biosynthesis of cofactors, carriers:biotin	2.5
cadA	b4131	Enzyme, degradation of small molecules: amino acids	2.2
cspG	b0990	Phenotype, not classified	2.5
edd	b1851	Enzyme, central intermediary metabolism: Entner-Douderoff	2.2
gadB	b1493	Enzyme, central intermediary metabolism: pool, multipurpose conversions	3.1
hdeA	b3510	Orf, unknown	2.9
hdeB	b3509	Orf, unknown	3.9
hdeD	b3511	Orf, unknown	2.3
inaA	b2237	Phenotype, adaptations, atypical conditions	5.6
marA	b1531	Regulator, drug/analog sensitivity	2.3
marR	b1530	Regulator, drug/analog sensitivity	2.7
mdaA	b0851	Phenotype, not classified	2.1
mdaB	b3028	Phenotype, not classified	2.1
rimK	b0852	Structural component, ribosomes–maturation and modification	2.5
ugpB	b3453	Transport, transport of small molecules: carbohydrates, organic acids, alcohols	2.2
ybjC	b0850	Orf, unknown	2.8
yddE	b1464	Orf, unknown	2.3
yeiR	b2173	Orf, unknown	2.4
yfaE	b2236	Orf, unknown	2.2
ygaC	b2671	Orf, unknown	2.7
yhbW	b3160	Putative enzyme, not classified	3.5
yhiX	b3516	Putative ARAC-type regulatory protein	3.4
yjgG	b4247	Orf, unknown	2.0

olism (*gadB*), transport (*ugpB*), and unknown functions (*b1165*, *hdeABD*, and *yhiX*). The DNA microarray results suggested that furanone has more of an effect on the genes positively regulated by AI-2 than those negatively regulated by AI-2, and the data corroborate that furanone inhibits the quorum-sensing related phenotype in *E. coli* (air–liquid biofilm discussed below) by blocking AI-2 signaling. Interestingly, some genes induced by furanone have functions for metabolism and stress response, such as *inaA* (involved in stress response), *marA* (encodes transcriptional activator of defense systems), and *ugpB* (involved in transport of small molecules); this suggested that furanone may affect the *E. coli* global stress response (although it does not affect its growth rate).

DNA Microarray Results Corroborated with RNA Dot Blotting

To validate the DNA microarray results, total RNA was isolated from four independent cultures and analyzed with RNA dot blotting. The same conditions were used as the AI-2^+ K12 vs. AI-2^- DH5α experiments as well as the same conditions of those with and without furanone; however, RNA was isolated independently from those RNA samples used in the DNA microarray experiments. Six genes were checked, *cheA*, *flgC*, *fliC*, *b1194*, *b1566*, and *yhjH*. The RNA dot blotting results of all these six genes agree with the DNA microarray results (Table IV); for example, *b1566* was induced 9- and 15-fold by AI-2 in the DNA microarray and RNA dot blotting experiments, respectively. Hence, the microarray results provide reliable information about the effects of AI-2 and furanone.

Escherichia coli AI-2 Concentration is Inhibited by Furanone

Previously, we showed that 5–10 μg/mL of furanone quenched the AI-2 signal of *E. coli* JM109: AI-2 activity was decreased up to 26,600-fold by adding furanone to supernatants containing AI-2 (Ren et al., 2001). To see if furanone altered *E. coli* K12 AI-2 concentrations, *E. coli* K12 was grown in 0.5X LB supplemented with 0.5% glucose and 0 or 100 μg/mL furanone. Furanone at 100 μg/mL has no effect on growth rate (1.91 h^{-1} without furanone vs. 1.82 h^{-1} with 100 μg/mL furanone). The cells were grown to OD = 0.9, then the supernatant was added to the reporter strain *V. harveyi* BB170 (10% v/v in AB medium), and the bioluminescence was measured 4 h after inoculation. It was found that 100 μg/mL furanone decreased AI-2 concentrations by 49% ± 7% (1.9×10^{-4} light units vs. 0.96×10^{-4} light units, normalized by cell numbers). This decrease in AI-2 concentration may explain partially the DNA microarray results in that the furanone repressed 67% of the genes (44 of 67 genes) induced by AI-2. Furanone present in the *E. coli* supernatant (10 μg/mL) had no effect on the growth of *V. harveyi* since the cell densities in the cultures with (3.7×10^7 cells/mL) and without furanone (3.4×10^7 cells/mL) were similar as shown by counting the CFU on the spread plates.

Air–Liquid Biofilm Formation of *E. coli* is Inhibited by Furanone

Bacteria have been known to move towards beneficial environments; for example, the cells use chemotaxis for chemical attraction, phototaxis for light attraction, and aerotaxis for oxygen attraction (Taylor et al., 1999). Besides the chemotaxis and flagellar genes found induced by AI-2 and repressed by furanone in the present study, it was an interesting discovery that *aer* (alternative name *air*, NCBI database) and *tsr* were also induced by AI-2 (5.3- and 28.4-fold, respectively, and repressed by furanone (4.6- and 18.1-fold, respectively, Table I). These two genes

Table IV. Comparison of gene expression changes by DNA microarray and RNA dot blotting.

Gene	Primers used for probe synthesis	Effect of AI-2		Effect of furanone (60 μg/mL)	
		Expression ratio (Microarray)	Expression ratio (Dot blot)	Expression ratio (Microarray)	Expression ratio (Dot blot)
flgC	5′-GGCCAGTAATCTGGCGAATGCTGAT-3′ 5′-ACCGAGCGTAAGGGTTTTCAGCATC-3′	+10	+50	−12.5	−50
fliC	5′-ACCGGTGGTGATAACGATGGGAAGT-3′ 5′-CTTCTGTTTTGCCATCATCTCCGCC-3′	+6	+100	−27	−20
b1194	5′-GGCAATAACCCCGGATAAACTGGTG-3′ 5′-CCCCATGTTGACTTCAATCTGAGCG-3′	+6	+30	−4	−20
b1566	5′-CCGTTATTTCAAACAACTCCGCCCC-3′ 5′-TGGTGCCAGCGGTATTTGTATCGTC-3′	+9	+15	−7	−20
yhjH	5′-TTATTCAGCGAATAAGCAACCCTGA-3′ 5′-ATATGCTCCACCAGTTCGAAACGCA-3′	+6	+10	−10	−100
cheA	5′-ACTCGATCAAAGGAGGGGCAGGAAC-3′ 5′-TGTCCCAGTTCTTCTTCCAGCAGGT-3′	+14	+40	−25	−15

encode signal transducers for aerotaxis (Rebbapragada et al., 1997).

E. coli has been well-studied for biofilm formation on different surfaces (Ghigo, 2001; Ren et al., 2001). However, *E. coli* K12 does not form good biofilms due to the absence of the conjugative F factor, which has been shown to stimulate biofilm formation (Ghigo, 2001; Reisner et al., 2003). Recently, we found F^+ *E. coli* JM109 could form an air–liquid interface biofilm as a ring around the wall of 96-well plates; hence, oxygen appears to be an attractant for this biofilm formation (the wells on the edge of 96-well plates also gave more biofilm, data not shown). To test if air–liquid biofilm formation is subject to regulation by AI-2 and furanone, *E. coli* JM109 was grown in 96-well plates and studied for its biofilm formation with different concentrations of furanone. JM109 has been reported to have AI-2 activity (Surette and Bassler, 1998), and this was confirmed in the present study (400-fold higher AI-2 activity than sterile LB medium, 3×10^{-5} light units vs. 7.3×10^{-7} light units). Since glucose stimulates AI-2 production and *E. coli* grown in LB without glucose does not produce AI-2 (Surette and Bassler, 1998), LB medium with or without supplemented glucose was used to create AI-2 positive or negative conditions. Previously, 0.1% glucose has been shown to stimulate AI-2 synthesis while 0.5% glucose gave the maximum AI-2 activity (Surette and Bassler, 1998). Hence, LB medium supplemented with 0, 0.2, 0.5, and 1.0% glucose was tested for *E. coli* JM109 biofilm formation. More biofilm was obtained when cells were grown with 0.2% glucose than with 0.5% or 1.0% glucose; therefore, LB supplemented with 0.2% glucose was used to generate an AI-2 positive environment to study the effect of furanone on biofilm formation. The total cell density (including both suspension and biofilm cells) was around an OD at 620 nm of 0.3 at 16 h after inoculation. It then increased with time until an OD at 620 nm around 0.6 at the end of the experiments (48 h after inoculation). This is similar for all the samples tested, and this range of cell density has been known to be optimum for AI-2 production (Surette and Bassler, 1998; Xavier and Bassler, 2003).

In the LB medium without supplemented glucose, the biofilm mass increased and reached maximum 16 h after inoculation. The biofilm mass fluctuated (within 30%) for the next 24 h, and reached a plateau 40 h after inoculation. In the LB medium supplemented with 0.2% glucose, however, the biofilm mass steadily increased and also reached a relative plateau 40 h after inoculation. By comparing biofilms grown with and without glucose (both without furanone) at 48 h after inoculation, it was found that AI-2 (synthesized via glucose addition) up-regulated biofilm formation 2.4-fold (Fig. 1). The biofilms grown with furanone have the same trend as those without furanone; however, furanone significantly inhibited biofilm formation. For example, 25, 50, 100 μg/mL furanone inhibited 10, 30, 51% of biofilm formation, respectively, in LB medium supplemented with 0.2% glucose (Fig. 1). Similar inhibition was obtained in LB medium without glucose (Fig. 1). Overall, the results showed that the furanone repressed the *E. coli* JM109 air–liquid interface biofilm formation, and AI-2 synthesis via glucose appeared to up-regulate biofilm formation. Hence, these results also indicated furanone acts to alter quorum sensing related phenotypes by inhibiting the same genes as AI-2.

DISCUSSION

In this study, we have shown clearly that furanone represses the same suite of genes positively controlled by AI-2, since 79% of genes repressed by furanone were also induced by AI-2. The two prior studies (DeLisa et al., 2001b; Sperandio et al., 2001) about *E. coli* gene expression affected by AI-2 gave very different results. Although the two strains (*E. coli* K12 wild-type and DH5α)

used in the AI-2 study here are not isogenic and these genetic differences may affect some aspects of the gene expression profile, the induction of chemotaxis, motility, and flagellar genes in our study agrees well with the result of Sperandio et al. (2001); hence, the present study was informative in identifying the AI-2-controlled genes and has served to elucidate the major effects of furanone in regard to AI-2 signaling, which was our main goal. The results reported here support our previous report that furanone inhibits quorum sensing of *E. coli* (Ren et al., 2001) and indicates that the inhibition was through the AI-2 signaling system. The unknown genes induced by the presence of AI-2 and repressed by furanone are of particular interest in terms of trying to control quorum sensing-related phenotypes such as biofilm formation and virulence. Overall, our results suggest that the furanone has specific inhibition on AI-2 quorum sensing regulon.

As expected, there are discrepancies for the two existing reports using DNA microarrays to study gene regulation by AI-2 (DeLisa et al., 2001b; Sperandio et al., 2001). For example, the report of Sperandio et al. (2001) found 10% of *E. coli* genes are under the control of AI-2, while DeLisa et al. (2001b) found 5.6% genes are controlled by AI-2. Both research groups found a number of genes for growth and cell division were differentially expressed in AI-2^+ and AI-2^- strains (22 and 23 genes, respectively); however, only one gene (*ftsE*) was consistent between the two reports. Also, the expression of some genes is conflicting; for example, the chemotaxis gene *cheW* was induced threefold by AI-2 in the report of Sperandio et al. (2001), but was repressed 2.7-fold in the report of DeLisa et al. (2001b). The differences between the two existing studies could be caused by the different growth conditions; e.g., the results of Sperandio et al. were obtained by comparing gene expression of AI-2^+ and AI-2^- strains grown to an OD of 1.0, while the data of DeLisa et al. were obtained by contacting a *luxS* mutant with AI-2^+ or AI-2^- supernatant. The difference could also be the result of the normalization procedures or noise in data. Our data are more similar with those in the report of Sperandio et al. (2001) in that AI-2 induces genes for chemotaxis, flagellar synthesis, and motility as evidenced by many genes of the same operons affected in a similar manner such as *fliACDFHIKMNOPQ*, *flgAM*, *motAB*, *cheABWYZ*, and *tar*.

It should be noted that the *E. coli* microarrays used in the previous studies and our study are all based on the sequence of *E. coli* K12 (DeLisa et al., 2001b; Sperandio et al., 2001). The *E. coli* O157:H7, used in the study of Sperandio et al., has 1.34 Mbp extra DNA that are absent in K12, and lacks 0.53 Mbp DNA, which are present in K12 (Sperandio et al., 2001). This is a significant difference (1.87 Mbp) given the size of *E. coli* K12 genome is 4.6 Mbp (Blattner et al., 1997; Sperandio et al., 2001). The strains used by DeLisa et al. were *E. coli* K12 derivatives, *E. coli* W3110 and its *luxS* mutant (DeLisa et al., 2001b). However, the data in the study of DeLisa et al. (2001b) are not uniformly consistent as the genes in the same operons were not consistently induced/repressed. For example, the expression ratios of *motA* and *motB* were −1.1 and +3.1, respectively.

In a previous study, Manefield et al. (1999) found 4-bromo-5-(bromomethylene)-3-(1-hydroxybutyl)-2(*5H*)-furanone induced six proteins and repressed six proteins in *E. coli* carrying *luxR* and *luxCDABE* gene on a plasmid. Eight of the twelve proteins were known proteins and five of these eight proteins were *E. coli* proteins (the other three, LuxA, LuxB, and LuxD, were from the cloned plasmid) (Manefield et al., 1999). None of genes encoding these five proteins was seen in the results of the present study (they were all expressed but not induced or repressed more than the cut-off ratios of 2.5 and 2 for AI-2 and furanone results, respectively). This is probably because the study of Manefield et al. (1999) was based on AHL signaling but the present study was to investigate the inhibition of AI-2 signaling. Also the furanone in the study of Manefield is slightly different from the one used in the present study [(*5Z*)-4-bromo-5-(bromomethylene)-3-butyl-2(*5H*)-furanone (furanone)]. The furanone used in the present study has a butyl chain, while the one used in the study of Manefield et al. has a hydroxybutyl chain. In the present study, one largely uncharacterized gene, *b1566,* also known as *flaX* (Ide and Kutsukake, 1997), was induced 8.8-fold by AI-2 and repressed 7.1-fold by furanone. Its expression was dependent on the sigma factor for class 3 flagellar operons; however, the *flaX* mutant did not show a defect in motility (Ide and Kutsukake, 1997). By using DNA microarrays, we found recently that *b1566* was induced 8.3-fold during *E. coli* K12 biofilm formation on mild steel plates compared to suspension cells (data not shown). Therefore, additional study on this gene may discover its functions, which are possibly related to quorum sensing as shown in the present study.

Another two interesting, previously uncharacterized genes are *b1194* and *yhjH,* which were induced 6.3- and 6.0-fold by AI-2, and repressed 4.0- and 9.9-fold by furanone. The expression ratios of both genes have been confirmed with RNA dot blotting (Table IV). The BLAST search http://www.ncbi.nlm.nih.gov/) for *b1194* did not show apparent homology with characterized bacterial genes. The *yhjH* gene was found to have homology to several different sequences, such as those for hypothetical proteins in *Shigella flexneri* and *Yersinia pestis* KIM. Also, a putative conserved domain (EAL domain) of diguanylate phosphodiesterase was found in YhiH, suggesting the *yhjH* product may be a signaling protein that has the metal-binding site.

Biofilm formation at the air–liquid interface is a complex process. Motility has been shown to be important (Pratt and Kolter, 1998) and aerotaxis is found to play a role in the present study. Our finding that a large number of related genes (those with functions in chemotaxis, motility, flagellar synthesis, and aerotaxis) were both induced by AI-2 and repressed by furanone indicates that furanone inhibited phenotypes such as biofilm formation (Fig. 1) by

repressing the same genes that AI-2 up-regulated. This is consistent with our results that the air–liquid biofilm formation is up-regulated by AI-2 and repressed by furanone (Fig. 1). However, how these common genes are regulated and the steps in biofilm formation that each of them controls remains unknown. Compared to the clear inhibition of furanone on the air-liquid biofilm formation, the up-regulation of biofilm formation by AI-2 is less conclusive since the effects of AI-2 and glucose are difficult to discriminate. The presence of glucose may cause fundamental changes in cell metabolism (Garrett and Grisham, 1999) and consequently affect the biofilm formation. We expect this will be solved by direct addition of pure AI-2, which was not available when this study was conducted, and is still not available due to the difficulty in its extraction (Chen et al., 2002).

Our results indicate that the large number of genes that we have identified as part of the AI-2 quorum-sensing regulon are repressed by furanone. Similarly, Hentzer et al. (2003) found that in *P. aeruginosa* PAO1, which does not produce AI-2 (Winzer et al., 2002), 80% of the synthetic furanone-repressed genes are involved in AI-1 quorum sensing. So there is now genetic evidence that furanone represses both the known quorum-sensing systems and this agrees with our earlier studies in which we showed furanone quenches both the AI-1 and AI-2 signals (Ren et al., 2001). Also, in the present study, *luxS* and *pfs*, which encode the proteins for AI-2 production (Schauder et al., 2001), were not apparently affected by furanone and Hentzer et al. (2003) also showed the AI-1 gene clusters (*lasI lasR* and *rhlI rhlR*) were not apparently affected by synthetic furanone. Hence, furanones appear to inhibit quorum sensing post-transcriptionally. As evidence of this post-transcriptional interaction, with Dr. Sunny Zhou at Washington State University, we have found recently that furanone becomes covalently attached to the LuxS protein (unpublished data) and have shown here that the extracellular AI-2 concentration is decreased twofold. The direct interaction of furanone with AI-2 signaling is also evidenced by the DNA microarray results in the present study in that *rbsB*, a homolog of *luxP,* which encodes the AI-2 receptor in *V. harveyi* (Chen et al., 2002), was induced both by furanone (2.3-fold) and AI-2 (2.7-fold) as shown in Table I. This suggests that furanone may compete with AI-2 for the receptor; but, the binding of furanone may have certain post-transcriptional effects, which finally lead to the repression of AI-2 signaling.

The finding that AI-2 up-regulates the motility and taxis genes supports the possible role of AI-2 in pathogenesis. Hence, adding furanone, which repressed these genes, is a promising approach in controlling bacterial infections related to AI-2 activity. Furanone has been shown previously to inhibit swarming and biofilm formation of *E.* coli XL1-Blue with no effect on growth rate (Ren et al., 2001). However, *E. coli* XL1-Blue does not have AI-2 activity (Ren et al., 2001). In the present study, furanone also inhibited the air–liquid interface biofilm formation in LB medium without glucose, which was shown to be negative for AI-2 production (Surette and Bassler, 1998). These results suggest that furanone has a broader effect than just inhibiting AHL and AI-2 signaling, and the genes identified in this study should help discern the mechanism of inhibition of quorum sensing-phenotypes by furanone.

The authors thank Dr. James J. Sims at University of California, Riverside, for providing a furanone standard and for his suggestions on the synthesis process.

References

Bassler BL. 1999. How bacteria talk to each other: Regulation of gene expression by quorum, sensing. Curr Opin Microbiol 2:582–587.

Bassler BL, Wright M, Silverman MR. 1994. Multiple signaling systems controlling expression of luminescence in *Vibrio harveyi*: Sequence and function of genes encoding a second sensory, pathway. Molec Microbiol 13:273–286.

Beck von Bodman S, Majerczak DR, Coplin DL. 1998. A negative regulator mediates quorum-sensing control of exopolysaccharide production in *Pantoea stewartii,* subsp. *stewartii*. Proc Natl Acad Sci USA 95:7687–7692.

Beechan CM, Sims JJ. 1979. The first synthesis of fimbrolides, a novel class of halogenated lactones naturally occuring in the red seaweed *Delisea fimbriata* (Bonnemaisoniaceae). Tetrahedron Lett 19:1649–1652.

Blattner FR, Plunkett G III, Bloch CA, Perna NT, Burland V, Riley M, Collado-Vides J, Glasner JD, Rode CK, Mayhew GF, et al. 1997. The complete genome sequence of *Escherichia coli* K-12. Science 277: 1453–1462.

Cao J-G, Meighen EA. 1989. Purification and structural identification of an autoinducer for the luminescence system of *Vibrio harveyi*. T J Biol Chem 264:21670–21676.

Chen X, Schauder S, Potier N, Dorsselaer AV, Pelczer I, Bassler BL, Hughson FM. 2002. Structural identification of a bacterial quorum-sensing signal containing boron. Nature 415:545–549.

Davies DG, Parsek MR, Pearson JP, Iglewski BH, Costerton JW, Greenberg EP. 1998. The involvement of cell-to-cell signals in the development of a bacterial biofilm. Science 280:295–298.

DeLisa MP, Valdes JJ, Bentley WE. 2001a. Quorum signaling via AI-2 communicates the "metabolic burden" associated with heterologous protein expression in *Escherichia coli*. Biotechnol Bioeng 75:439–450.

DeLisa MP, Wu C-F, Wang L, Valdes JJ, Bently WE. 2001b. DNA microarray-based identification of genes controlled by autoinducer 2—Stimulated quorum sensing in *Escherichia coli*. J Bacteriol 183: 5239–5247.

Fawcett P, Eichenberger P, Losick R, Youngman P. 2000. The transcriptional profile of early to middle sporulation in *Bacillus subtilis*. Proc Natl Acad Sci USA 97:8063–8068.

Fong KP, Chung WO, Lamont RJ, Demuth DR. 2001. Intra- and interspecies regulation of gene expression by *Actinobacillus actinomycetemcomitans* LuxS. Infection and Immunity 69:7625–7634.

Garrett RH, Grisham CM. 1999. Biochemistry. Orlando, FL: Harcourt Brace & Company.

Ghigo J-M. 2001. Natural conjugative plasmids induce bacterial biofilm, development. Nature 412:442–445.

Gram L, de Nys R, Maximilien R, Givskov M, Steinberg P, Kjelleberg S. 1996. Inhibitory effects of secondary metabolites from the red alga *Delisea pulchra* on swarming motility of *Proteus mirabilis*. Appl Environ Microbiol 62:4284–4287.

Greenberg EP, Hastings JW, Ulitzur S. 1979. Induction of luciferase synthesis in *Beneckea harveyi* by other marine bacteria. Arch Microbiol 120:87–91.

Helmann JD, Wu MFW, Kobel PA, Gamo F-J, Wilson M, Morshedi MM, Navre M, Paddon C. 2001. Global transcriptional response of *Bacillus subtilis* to heat shock. J Bacteriol 183:7318–7328.

Hentzer M, Riedel K, Rasmussen TB, Heydorn A, Andersen JB, Parsek MR, Rice SA, Eberl L, Molin S, Høiby N, et al. 2002. Inhibition of quorum sensing in *Pseudomonas aeruginosa* biofilm bacteria by a halogenated furanone compound. Microbiology 148:87–102.

Hentzer M, Wu H, Andersen JB, Riedel K, Rasmussen TB, Bagge N, Kumar N, Schembri MA, Song Z, Kristoffersen P, et al. 2003. Attenuation of *Pseudomonas aeruginosa* virulence by quorum sensing inhibitors. Eur Molec Biol Org J 22:3803–3815.

Ide N, Kutsukake K. 1997. Identification of a novel *Escherichia coli* gene whose expression is dependent on the flagellum-specific sigma factor, FliA, but dispensable for motility development. Gene 199:19–23.

Li Y-H, Lau PCY, Lee JH, Ellen RP, Cvitkovitch DG. 2001. Natural genetic transformation of *Streptococcus mutans* growing in biofilms. J Bacteriol 183:897–908.

Lilley BN, Bassler BL. 2000. Regulation of quorum sensing in *Vibrio harveyi* by LuxO and Sigma-54. Molec Microbiol 36:940-954.

Lithgow JK, Danino VE, Jones J, Downie JA. 2001. Analysis of N-acyl homoserine-lactone quorum-sensing molecules made by different strains and biovars of *Rhizobium Leguminosarum* containing different symbiotic plasmids. Plant Soil 232:3–12.

Manefield M, de Nys R, Kumar N, Read R, Givskov M, Steinberg P, Kjelleberg S. 1999. Evidence that halogenated furanones from *Delisea pulchra* inhibit acylated homoserine lactone (AHL)-mediated gene expression by displacing the AHL signal from its receptor protein. Microbiology 145:283–291.

Manefield M, Harris L, Rice SA, de Nys R, Kjelleberg S. 2000. Inhibition of luminescence and virulence in the black tiger prawn (*Penaeus monodon*) pathogen *Vibrio harveyi* by intercellular signal antagonists. Appl Environ Microbiol 66:2079–2084.

Manefield M, Rasmussen TB, Hentzer M, Anderson JB, Steinberg P, Kjelleberg S, Givskov M. 2002. Halogenated furanones inhibit quorum sensing through accelerated LuxR turnover. Microbiology 148:1119–1127.

Manny AJ, Kjelleberg S, Kumar N, de Nys R, Read RW, Steinberg P. 1997. Reinvestigation of the sulfuric acid-catalysed cyclisation of brominated 2-alkyllevulinic acids to 3-alkyl-5-methylene-2(5H)-furanones. Tetrahedron 53:15813–15826.

McNab R, Ford SK, El-Sabaeny A, Barbieri B, Cook GS, Lamont RJ. 2003. LuxS-based signalling in *Streptococcus gordonii*:: Autoinducer 2 controls carbohydrate metabolism and biofilm formation with *Porphyromonas gingivalis*. J Bacteriol 185:274–284.

Pratt LA, Kolter R. 1998. Genetic analysis of *Escherichia coli* biofilm formation: Roles of flagella, motility, chemotaxis and type I pili. Molec Microbiol 30:285–293.

Rebbapragada A, Johnson MS, Harding GP, Zuccarelli AJ, Fletcher HM, Zhulin IB, Taylor BL. 1997. The Aer protein and the serine chemoreceptor Tsr independently sense intracellular energy levels and transduce oxygen, redox, and energy signals for *Escherichia coli* behavior. Proc Nat Acad Sci USA 94:10541–10546.

Reisner A, Haagensen JAJ, Schembri MA, Zechner EL, Molin S. 2003. Development and maturation of *Escherichia coli* K-12 biofilms. Molec Microbiol 48:933–946.

Ren D, Bedzyk L, Setlow P, Thomas S, Ye RW, Wood TK. 2004. Gene expression in *Bacillus subtilis* surface biofilms with and without sporulation and the importance of *yveR* for biofilm maintenance. Biotechnol Bioeng 86:344–364.

Ren D, Bedzyk L, Thomas S, Ye RW, Wood TK. 2004. Gene expression in *Escherichia coli*. Biofilms Appl Microbiol Biotechnol 64:515–524.

Ren D, Sims JJ, Wood TK. 2001. Inhibition of biofilm formation and swarming of *Escherichia coli* by (*5Z*)-4-bromo-5-(bromomethylene)-3-butyl-2(*5H*)-furanone. Environ Microbiol 3:731–736.

Ren D, Wood TK. 2004. (*5Z*)-4-bromo-5-(bromomethylene)-3-butyl-2(*5H*)-furanone reduces corrosion from *Desulfotomaculum orientis*. Environ Microbiol 6:535–540.

Sambrook J, Fritsch EF, Maniatis T. 1989. Molecular cloning, a laboratory manual. Cold Spring Harbor, NY: Cold Spring Harbor Laboratory Press.

Schauder S, Shokat K, Surette MG, Bassler BL. 2001. The LuxS-family of bacterial autoinducers: Biosynthesis of a novel quorum-sensing signal molecule. Molec Microbiol 41:463–476.

Schembri MA, Kjærgaard K, Klemm P. 2003. Global gene expression in *Escherichia coli*. Biofilms Molec Microbiol 48:253–267.

Shoemaker DD, Linsley PS. 2002. Recent developments in DNA microarray. Curr Opin Microbiol 5:334–337.

Sperandio V, Torres AG, Giron JA, Kaper JB. 2001. Quorum sensing is a global regulatory mechanism in enterohemorrhagic *Escherichia coli* O157:H7. J Bacteriol 183:5187–5197.

Stanley NR, Britton RA, Grossman AD, Lazazzera BA. 2003. Identification of catabolite repression as a physiological regulator of biofilm formation by *Bacillus subtilis* by use of DNA microarrays. J Bacteriol 185:1951–1957.

Stintzi A, Evans K, Meyer J-M, Poole K. 1998. Quorum-sensing and siderophore biosynthesis in *Pseudomonas aeruginosa*: *lasR/lasI* mutants exhibit reduced pyoverdine biosynthesis. FEMS Microbiol Lett 166:341–345.

Surette MG, Bassler BL. 1998. Quorum sensing in *Escherichia coli* and *Salmonella typhinurium*. Proc Natl Acad Sci USA 95:7046–7050.

Surette MG, Miller MB, Bassler BL. 1999. Quorum sensing in *Escherichia coli*, *Salmonella typhimurium,* and *Vibrio harveyi*: A new family of genes responsible for autoinducer production. Proc Natl Acad Sci USA 96:1639–1644.

Taga ME, Semmelhack JL, Bassler BL. 2001. The LuxS-dependent autoinducer AI-2 controls the expression of an ABC transporter that functions in AI-2 uptake in *Salmonella typhimurium*. Molec Microbiol 42:777–793.

Taylor BL, Zhulin IB, Johnson MS. 1999. Aerotaxis and other energy-sensing behavior in bacteria. Ann Rev Microbiol 53:103–128.

Wei Y, Lee J-M, Richmond C, Blattner FR, Rafalski JA, Larossa RA. 2001. High-density microarray-mediated gene expression profiling of *Escherichia coli*. J Bacteriol 183:545–556.

Whiteley M, Bangera MG, Bumgarner RE, Parsek MR, Teltzel GM, Lory S, Greenberg EP. 2001. Gene expression in *Pseudomonas aeruginosa* biofilms. Nature 413:860–864.

Wilson M, DeRisi J, Kristensen H-H, Imboden P, Rane S, Brown PO, Schoolnik GK. 1999. Exploring drug-induced alterations in gene expression in *Mycobacterium tuberculosis* by microarray hybridization. Proc Natl Acad Sci USA 96:12833–12838.

Winzer K, Hardie KR, Burgess N, Doherty N, Kirke D, Holden MTG, Linforth R, Cornell KA, Taylor AJ, Hill PJ, Williams P. 2002. LuxS: Its role in central metabolism and the in vitro synthesis of 4-hydoxy-5-methyl-3(*2H*)-furanone. Microbiology 148:909–922.

Xavier KB, Bassler BL. 2003. LuxS quorum sensing: More than just a numbers game. Curr Opin Microbiol 6:191–197.

Ye RW, Tao W, Bedzyk L, Young T, Chen M, Li L. 2000. Global gene expression profiles of *Bacillus subtilis* grown under anaerobic conditions. J Bacteriol 182:4458–4465.

Zheng M, Wang X, Templeton LJ, Smulski DR, LaRossa RA, Storz G. 2001. DNA microarray-mediated transcriptional profiling of the *Escherichia coli* response to hydrogen peroxide. J Bacteriol 183:4562–4570.